Journal of The Electrochemical Society, **149** (3) A319-A324 (2002)
0013-4651/2002/149(3)/A319/6/$7.00 © The Electrochemical Society, Inc.

Electrodeposited Tin Coating as Negative Electrode Material for Lithium-Ion Battery in Room Temperature Molten Salt

Y. S. Fung*,z and D. R. Zhu

Department of Chemistry, The University of Hong Kong, Hong Kong SAR, China

A new room temperature molten salt (RTMS) [1-methyl-3-ethylimidazolium/$AlCl_3$/$SnCl_2$ (3:2:0.5)] was developed for depositing tin on a copper electrode. Different tin crystallites were deposited at different temperatures, giving widely different performances of the assembled lithium cell [Sn (Cu)/LiCl buffered MEICl-$AlCl_3$ RTMS/lithium]. Tin film deposited at 50°C or higher gave a more desirable crystal structure and an improved performance than films obtained at lower temperatures. Both cyclic voltammetry and galvanostatic cycling show the formation of three major lithium-tin alloy phases corresponding to the phase transition of LiSn/Li_7Sn_3, $Li_{13}Sn_5$/Li_7Sn_2, and Li_7Sn_2/$Li_{22}Sn_5$. Increases in the charging and discharging capacities were found with the deposition of higher lithium-rich tin alloys, though at the degradation of the irreversible capacity at the first cycle. The discharging capacity decreased rapidly, producing loose, expanded, and irregular crystallites upon cycling at a high current density (cd) (1.0 mA/cm^2). However, an average capacity of 140 mAh/g, coulombic efficiency around 85%, and more than 200 cycles were obtained at a low cd (0.4 mA/cm^2). The improvement is attributed to the deposition of small and regular tin crystallites that allows reversible insertion and removal of lithium from a more stable crystal structure without a significant volume change during cycling.
 [DOI: 10.1149/1.1448501]

Manuscript submitted June 11, 2001; revised manuscript received October 16, 2001. Available electronically February 5, 2002.

Room temperature molten salts (RTMS) based on 1-methyl-3-ethylimidazolium chloride (MEICl) have been shown to provide an interesting ionic medium for battery applications and for alloy electrodeposition.[1-6] Since the successful introduction of a high concentration of lithium ion into the melts[7-11] by adding an excess amount of solid LiCl into the Lewis acidic $AlCl_3$-MEICl melts to form buffered neutral molten salts, the pace of development of the MEICl system for the lithium-ion battery has been increased recently. This is attributed to several desirable features of the system as an electrolyte for a lithium battery such as nonflammability, improved lithium conductivity, and a wide electrochemical window.[7-9]

Materials intercalated with lithium ions such as $LiCoO_2$, $LiMn_2O_4$, and $LiNiO_2$ have been used successfully as positive electrode materials in RTMS in previous studies.[10,11] However, a suitable negative electrode material for the lithium battery is more difficult to find in RTMS. Although carbonaceous materials had been widely investigated as intercalation anodes for lithium-ion secondary battery in the organic electrolyte system, their application as anode material in RTMS led to a very serious exfoliation problem due to the irreversible cointercalation of other ions present in the melt that reduced the subsequent performance of the anode during cycling. Moreover, as the potential of the lithium-intercalated carbon electrode is within 10 mV of that of the lithium metal, concerns have been raised about the safety of the negative electrode. Thus, metals capable of alloying reversibly with lithium were studied as the negative electrode material in RTMS. The most common metal chosen is aluminum which had been used as the negative electrode in our previous studies.[10,11] The problem with aluminum was the rather large volume expansion during alloying with lithium that led to the breakdown of the electrode structure upon repeated cycling.[10,11]

Recently, attention has been given to lithium-tin alloys or oxides that utilized the reversible reaction of lithium with tin because they offered high capacity, low capacity fade, and good safety properties.[12-14] A high irreversible capacity was observed during the first cycle in the use of the tin oxide negative electrode, and this precluded its commercial use.[15] To mitigate the irreversible capacity associated with tin oxides, Metallic electrodes such as tin alloys or other tin composites[16,17] have been employed directly as the negative electrode. The metallic tin electrode offered a promising anode material for lithium batteries due to its good mechanical properties. Thus, it was selected for studying its performance in RTMS for lithium battery application in the present work.

As different forms of tin metal had been shown to exhibit a strong effect on their electrochemical performance in lithium battery,[18] methods for the fabrication of the tin working electrode were investigated to obtain tin deposits of suitable forms for battery operation in RTMS. The procedure for the electrochemical deposition of a thin film of tin on the copper substrate as a current collector was adopted in the present study to develop an anode with a high current capacity. As RTMS was used as the medium for the development of the lithium battery in the present study, it was chosen as the electrolyte for the deposition of a tin film on the copper substrate, followed by a detailed study of its electrochemical and cycling behavior in RTMS.

In this paper, the development of a novel procedure for depositing a suitable tin film in RTMS for lithium-ion battery application is given. Factors affecting the quality of the tin film deposit have been investigated, and the optimized working conditions studied. Results on the electrochemical performance of the tin film electrode for lithium battery application are presented and discussed. The performance of a secondary lithium battery in RTMS incorporating the thin tin film as one of the electrodes is reported and its suitability as anode material discussed.

Experimental

Room temperature molten salts.—The MEICl was synthesized as previously described.[1-7] The MEICl/$AlCl_3$ melts (RTMS) was prepared by slowly adding a calculated amount of $AlCl_3$ (Aldrich, 99.99%) to the MEICl in a glove box under a positive pressure of argon. The $SnCl_2$ and LiCl were dehydrated under vacuum at 180°C for 10 h prior to use. The electrolyte for the electrodeposition of Sn was prepared by adding calculated amounts of $SnCl_2$ to the basic RTMS with a mole ratio of 3:2. All compositions of RTMS in this paper are expressed as mole ratios unless indicated otherwise. The LiCl buffered neutral RTMS was prepared by adding a calculated amount of solid LiCl into the acidic RTMS to form a melt with mole ratios of 1:1.2:0.2 and stirred for several days until all the LiCl had dissolved. Then about 5% of the excess buffering solid LiCl was added to the melts to produce the buffered neutral melts. The electrodeposition of Sn was conducted in a RTMS consisting of MEICl/$AlCl_3$/$SnCl_2$ in mole ratios of 3:2:0.5, respectively.

* Electrochemical Society Active Member.
z E-mail: ysfung@hkucc.hku.hk

Instrumentation.—All electrochemical experiments were performed by an EG&G software-controlled (EG&G model 270) PAR model 263 potentiostat/galvanostat and conducted inside an argon-filled glove box. The specific conductivity was measured by the EG&G model 5210 lock-in amplifier and 398 software at 100 kHz using a DJS-1 conductivity electrode. The Cambridge model 360 Stereoscan scanning electron microscope (SEM) and the Perkin Elmer model 3110 atomic absorption spectrometer (AAS) were used for analysis of the morphology and chemical composition of the tin deposit on the copper electrode. The charging-discharging experiments were conducted by a homemade constant current device controlled by a microcomputer with software written in the Basic program.

Cells and electrodes.—All electrochemical experiments were conducted in an electrochemical cell using an Al wire in the acidic RTMS ($AlCl_3$:MEICl = 66.7:33.3) as the reference electrode and an aluminum foil (6 × 5 mm) as the counter electrode. Copper foil (Aldrich, 0.127 mm thick, 99%) was used as the working electrode with one side of the surface covered by a Teflon adhesive tape so as to expose a known area (6 × 5 mm) to the RTMS. The electrochemical cell was placed on a copper furnace inside the glove box with a controlled temperature from 22 to 120°C by a Eurotherm model 1428 temperature controller.

The copper working electrode was polished using abrasive silicon carbide papers P 220, P 1000, and P 1600 in sequence before washing with acetone and drying in vacuum prior to use. After coating a thin film of Sn without stirring under the selected potential or constant current in the MEICl/$AlCl_3$/$SnCl_2$, the copper electrodes were rinsed immediately in acetonitrile and dried in the dry box directly. It was then assembled as a negative electrode in the lithium cell, Sn(Li)/LiCl buffered RTMS/Lithium foil, for performing the cycling experiments.

Chemical composition analysis.—After the deposition of Sn, the copper electrodes were immediately rinsed thoroughly in acetonitrile and dried in the dry box. The morphology of the deposits was investigated using the SEM and their chemical composition determined by the energy dispersive X-ray (EDX) microprobe. The total amount of Sn in the coating was determined by dissolving the deposits in 10 mL 1% HNO_3 solution prior to chemical analysis using an AAS.

Results and Discussion

Deposition of a thin film of tin on copper in RTMS.—The RTMS system based on MEICl/$AlCl_3$ provides a suitable medium for the electrodeposition of tin, as its amphoteric property can be utilized to assist its dissolution in RTMS by adjusting the acidity of the RTMS via the acidic $AlCl_3$ and basic MEICl interaction. When $SnCl_2$ or other acidic transition metal chloride is added to the basic melts, it can undergo the following coordination reaction with the free Cl^- present in RTMS as shown in

$$SnCl_2 + pCl^- \rightarrow [SnCl_{p+2}]^{p-} \qquad [1]$$

Thus, $SnCl_2$ can be dissolved into the ternary MEICl/$AlCl_3$/$SnCl_2$ melt by adding $SnCl_2$ to the basic binary melt MEICl/$AlCl_3$ with the excess free Cl^- coming from MEICl. A considerable amount of $SnCl_2$ were found to be incorporated in the ternary melt using this procedure. To provide a suitable medium for the electrodeposition of tin, the ternary melt must contain a high concentration of $SnCl_2$ and show good conductivity at a suitable temperature. The basic molten salt MEICl/$AlCl_3$ with a mole ratio of 3:2 was chosen as the base melt for the incorporation of $SnCl_2$ to form the ternary melt. The variation of the specific conductivity of the melts at different mole fractions of $SnCl_2$ in the 3:2 MEICl/$AlCl_3$ melt is shown in Fig. 1. The lowest conductivity had been observed at 5 mS/cm for the binary melt at 22°C and the highest conductivity at 43 mS/cm was obtained near the neutral

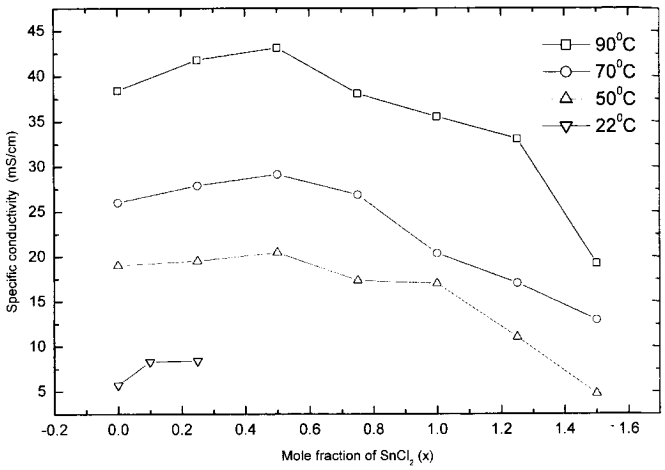

Figure 1. The variation of the specific conductivity of the ternary molten salts MEICl/$AlCl_3$/$SnCl_2$(3:2:x) on the mole fraction x of $SnCl_2$ at different temperatures.

composition of the ternary melts at mole fractions of 3:2:0.5. The conductivity is in general increased with the mole fraction of $SnCl_2$ until 0.5 and gradually declined at higher mole fractions. This is in agreement with the previous observation that the highest specific conductivity was obtained at neutral melts.[19] Thus, a ternary melt of MEICl/$AlCl_3$/$SnCl_2$ (3:2:0.5) was selected as the medium for the electrodeposition of tin.

The widely used copper foil was chosen as the substrate for the electrodeposition of tin due to its availability, good electric conductance, and inertness for alloying with tin. The electrochemical behavior of the copper electrode in MEICl/$AlCl_3$/$SnCl_2$ (3:2:0.5) was studied using cyclic voltammetry (CV). The cyclic voltammogram shown in Fig. 2 exhibits a single reduction wave near −1.0 V followed by a broad oxidation wave at −0.65 V. The reduction current starts to increase from the baseline at −0.72 V, and when the copper electrode was controlled at a value more negative than this potential, a gray film was found to appear at the copper substrate. Results of XRD analysis of the film indicated the existence of tin metal by showing two peaks at diffraction angles (2θ) of 30.6 and 32.0°.[20] Thus, the reduction current starting at −0.72 V was attributed to the reduction of Sn(II) to tin metal. It was interesting to note that a

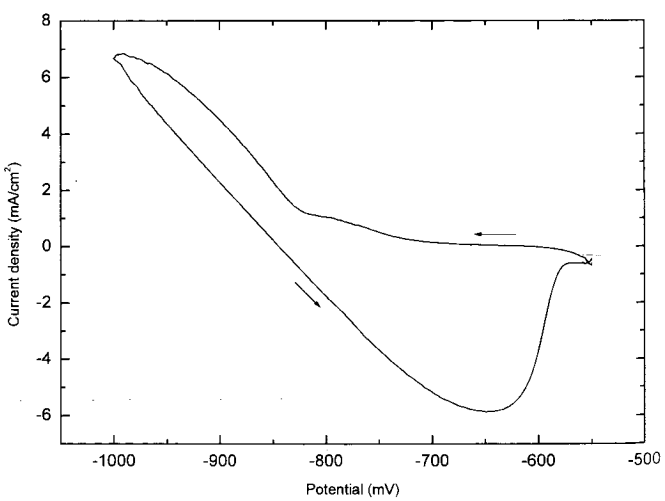

Figure 2. Cyclic voltammogram for a copper electrode in the MEICl/$AlCl_3$/$SnCl_2$(3:2:0.5) melts at a scan rate of 20 mV/s. Temperature: 50°C.

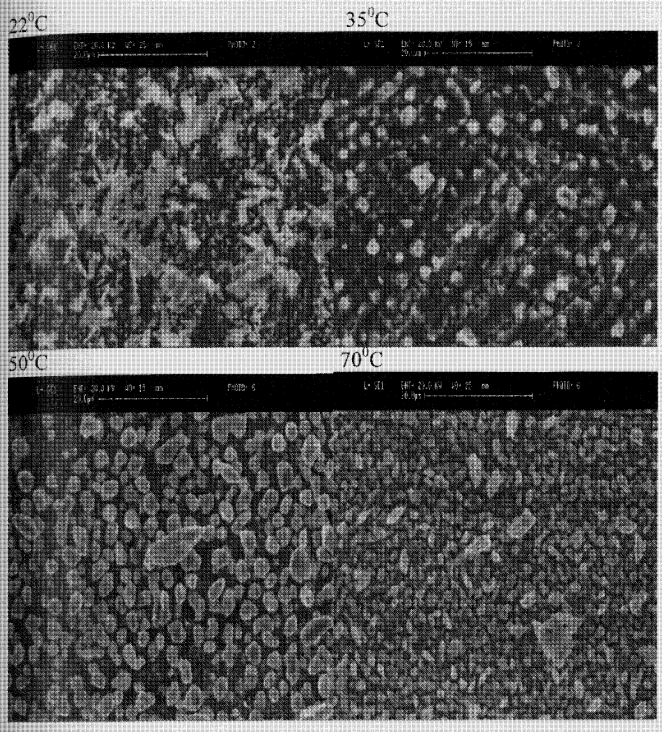

Figure 3. SEM micrographs of tin film deposited at different temperatures at a constant current density of 3.3 mA/cm^2.

marked increase in the reduction current was observed at potentials more negative than −0.82 V. Moreover, dendrites were found to deposit easily near the edge of the substrate when the potential was kept more negative than −0.9 V. Thus, it can be concluded that the marked increase in current was caused by a rapid increase in the electrode area at a negative potential as the result of a dendritic outgrowth of the tin deposits. To avoid uncontrollable deposition and the formation of an unstable electrode structure, the deposition potential was set to be more positive than −0.9 V to prevent the formation of dendrites. Therefore, a constant current density of 3.3 mA/cm^2 was chosen to keep the average deposition potential near −0.85 V.

The effect of temperature on the deposition of tin on the copper electrode in the MEICl/$AlCl_3$/$SnCl_2$ (3:2:0.5) melt was investigated using a constant current density of 3.3 mA/cm^2 at temperatures ranging from 22 to 70°C. SEM was used to study the particle size and surface morphologies of the deposited Sn film, and the results are shown in Fig. 3. At low deposition temperatures (22 and 35°C), dendritic and large elongated tin crystallites were found. As the temperature was increased, the deposited tin crystals became more regular. The grain size of the Sn crystallites was found to decrease at a higher temperature, showing an average size of 4 μm at 50°C and 2 μm at 70°C. The distribution of the Sn crystallites at the copper electrode was found to be homogeneous as shown by the dot mapping and results of the EDX elemental analysis of tin. The results indicate that the morphology of the tin crystals is highly dependent on the temperature of the melt during electrodeposition, and the electrochemical performance of the thin film tin electrode is highly affected by its morphology. Controlling the melt at a temperature of 50°C during tin deposition was found to produce a more uniform particle distribution and round-shaped crystallites that have been found suitable for the insertion of lithium as shown by results given in the next section. However, too high a temperature could lead to the formation of smaller, though still regular, crystallites. This may be the balancing effect of crystal growth against nucleation. In view

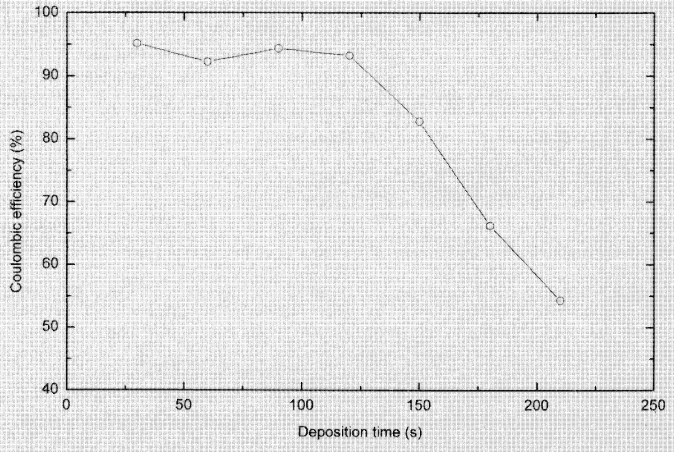

Figure 4. The effect of the deposition time at a constant current density of 3.3 mA/cm^2 on the coulombic efficiency for the electrodeposition of tin in RTMS at 50°C.

of the formation of large, regular crystallites, temperature at 50°C was selected for the deposition of tin on copper to produce the tin electrode for subsequent studies.

As the thickness of the tin film was controlled by the deposition time, *i.e.*, the total coulombs passed during electrodeposition, the effect of the deposition time on the coulombic efficiency was studied in RTMS at 50°C under a constant current density of 3.3 mA/cm^2 with an average deposition potential at about −0.85 V. The coulombic efficiency for Sn deposition was calculated as $Q_{Sn}/Q_{Total} \times 100\%$. Q_{Sn} was the charge estimated from the deposited mass of Sn by the results of AAS analysis, and Q_{Total} was the total quantity of charge passed during the electrodeposition. The results are shown in Fig. 4. The coulombic efficiency was kept larger than 90% up to a deposition time of 120 s or 400 mC/cm^2 and decreased rapidly when more than 400 mC/cm^2 were deposited. A lot of dendrites were observed when more coulombs, due to tin deposition, were passed. Thus, a deposition time of 120 s at 3.3 mA/cm^2 was chosen for the preparation of the tin film electrode for subsequent studies.

Deposition of lithium on tin film electrode in RTMS.—To study the electrochemical insertion of lithium into the tin film electrode, a tin film electrode was prepared by procedures as described in the previous section. After Sn deposition, the electrode was rinsed rigorously by anhydrous acetonitrile and dried for a few minutes in the dry box before use as the negative electrode for the RTMS lithium battery. It was then used directly for the electrochemical investigation in the LiCl buffered neutral molten salts (MEICl:$AlCl_3$:LiCl = 1:1.2:0.2) that was used as the electrolyte for battery application in previous studies.[10,11] First, CV was used to study the kinetics for the deposition of lithium on a pure copper electrode in LiCl buffered RTMS with results shown in Fig. 5. For lithium deposition at the copper electrode, a large cathodic peak was found to appear at a potential of −2.0 V followed by a couple of small anodic peaks during stripping at the first scan (Fig. 5). At the second scan, the cathodic current was greatly suppressed, and the stripping peaks almost disappeared. A black film was found at the surface of the copper electrode after several scans. Results of the EDX microanalysis of the film showed the existence of a Cl element in addition to the copper peak. This indicates that lithium has been deposited during the first CV scan with a low stripping efficiency. It is possible that the highly reactive lithium deposit could react with components in the melt to form a passivated LiCl film that prevents further lithium deposition in subsequent CV scans.

The cyclic voltammograms for the Sn film electrode were found to be highly dependent on the temperature for the deposition of the tin film. For a tin film deposited at 22°C, its CV scan in the LiCl

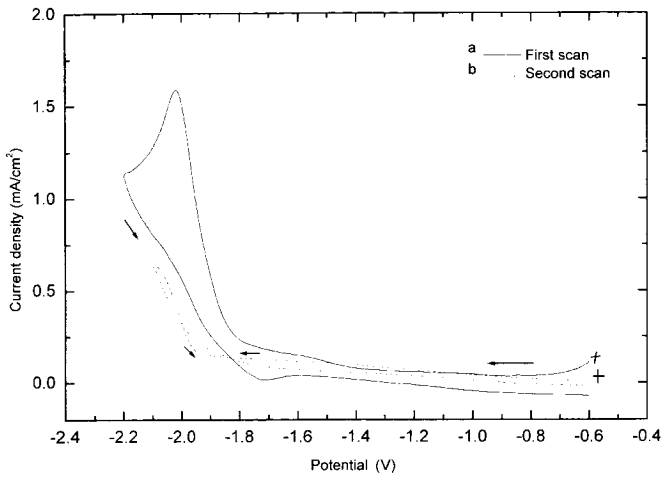

Figure 5. Cyclic voltammogram of a copper electrode in the LiCl buffered RTMS at a scan rate of 20 mV/s. The second scanning was conducted after a rest time of 1 min. Temperature: 22°C.

buffered RTMS electrolyte is shown in Fig. 6. Only a rising current for cathodic deposition was observed without any trace of stripping current during the reverse scan. However, when the deposition temperature was increased to 50°C, stripping peaks were found to appear in the voltammograms as shown in Fig. 7. When the scan potential was reversed at −1.65 V, a deposition peak appeared at −1.55 V together with a stripping peak at −1.3 V. When the switching potential was further extended to −2.1 V, two more deposition peaks appeared at −1.9 and −2.0 V in addition to the existing deposition peak at −1.65 V. Three corresponding stripping peaks were found at −1.5, −1.4, and −1.3 V. The results indicated the formation of three different types of lithium-tin alloys corresponding to the three couples of deposition and stripping peaks. This was in agreement with results reported in the literature[21] on the phase diagram of the lithium-tin system that showed three major lithium-tin alloy phases corresponding to the two-phase transition for $LiSn/Li_7Sn_3$, $Li_{13}Sn_5/Li_7Sn_2$, and $Li_7Sn_2/Li_{22}Sn_5$ among the six intermediate phases.

The reason for the appearance of Li/Sn alloys only on Sn crystallites produced at high temperature may due to the difference of the Sn crystals formed. Bigger and more regular tin crystallites deposited on the copper electrode at temperatures higher than 50°C allowed the diffusion of lithium into its crystal lattice to form various Li-Sn alloys as shown by the results given in Fig. 3. For the

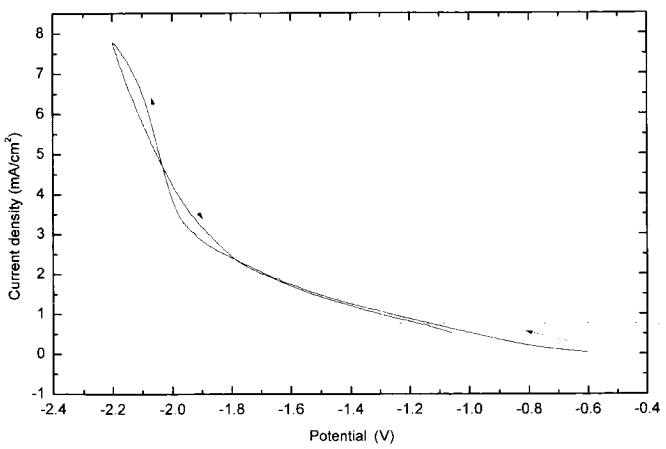

Figure 6. Cyclic voltammogram for a tin film electrode deposited at 22°C in the LiCl buffered RTMS at a scan rate of 20 mV/s. Temperature: 22°C.

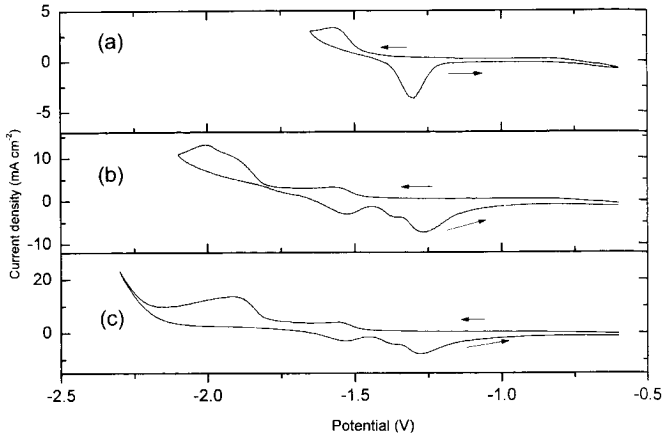

Figure 7. Cyclic voltammograms for tin film electrodes in the LiCl buffered RTMS at a scan rate of 20 mV/s. Tin films were plated at 50°C. Switching potentials are: (a) −1.62, (b) −2.1, and (c) −2.3 V. Temperature: 22°C.

deposition at 22°C, the tin deposits were dendritic in appearance, and the crystallites produced could not form Li/Sn alloys during lithium deposition, possibly due to the restriction in the crystal lattice. Thus, the tin film electrode should be formed at 50°C, if it is going to be used as a negative electrode in lithium-ion battery and the high temperature Sn electrodes were used in subsequent cycling studies.

Cycling study of a RTMS cell with a Sn film negative electrode.—The first five galvanostatic cycles of a RTMS cell (Sn(Li)/RTMS ($MEICl:AlCl_3:LiCl$ = 1:1.2:0.2)/Li) at room temperature (22°C) are shown in Fig. 8. The cycling was controlled at cell voltage limits between 0.1 and 1.0 V *vs.* lithium. The potentials for the first cycle show plateaus at 0.38, 0.23, and 0.15 V in the charging (or lithium deposition) curve corresponding to the three major peaks for the two-phase regions as observed in the CV voltammogram (Fig. 7). The subsequent cycles showed a reduced

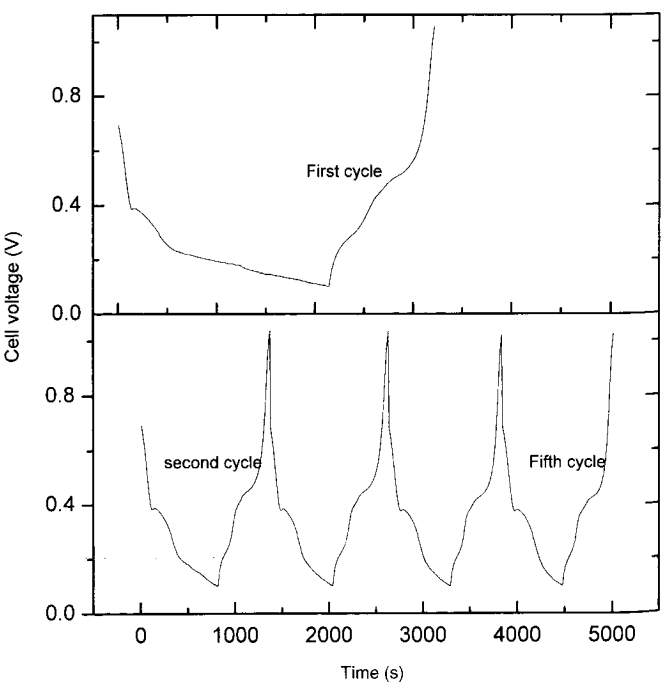

Figure 8. The first five galvanostatic cycles under a constant cd at 0.4 mA/cm² for a RTMS cell [Sn(Cu)/LiCl buffered RTMS/lithium foil].

Table I. The irreversible capacity obtained in the first cycle for the Li_xSn/RTMS/Li cells charging to different depths to deposit various lithium-tin alloys.

Cell	Li_xSn[b]	First cycle capacity (mAh/g)[a] Charging	Discharging	Irreversible capacity, $Q_{irrev.}$ (mAh/g)	% $Q_{irrev.}$
1	LiSn	225	160	65	28.9
2	$Li_{2.4}Sn$	541	271	270	49.9
3	$Li_{3.5}Sn$	790	289	501	63.4
4	$Li_{4.4}Sn$	993	305	688	69.3

[a] Charging-discharging current density = 0.4 mA/cm^2.
[b] Deposited at constant current charging to different depths in the first cycle to form specified lithium-tin alloys according to the coulombic calculation.

charging/discharging curve (Fig. 8) as compared to the first cycle, indicating that lithium was taken up during the initial development of the lithium-tin alloy electrode during cycling. The loss of capacity during cycling may due to the following reasons: (*i*) corrosion of the reactive alloys with impurities present in the melt, (*ii*) some lithium metals are needed in order to develop the electrode initially by alloying with tin, and (*iii*) there may be side reactions occurring at the surface of the tin electrode.

To investigate the effect of the appearance of different phases of Li-Sn at the electrode surface on the development of the lithium-tin alloy electrode, the first cycle charging was performed at different depths corresponding to the appearance of selected Li-Sn phases by coulombic calculation. The results are shown in Table I. The charging and discharging capacity were calculated as the total amount of coulombs delivered to or extracted from the tin film electrode during the formation of the Sn-Li alloy electrode. In general, both the charging and discharging capacities were found to increase with the deposition of Li-Sn alloys with higher lithium activities. However, the irreversible capacity at the first cycle is also increased at the same time, indicating that more lithium is needed for the development of the tin film electrode for initial cycling at a higher voltage.

As a higher cell voltage is desired for the lithium battery, cycling up to the formation of $Li_{22}Sn_5$ was investigated for extended cycling with results given in Table II. The coulombic efficiency was calculated based on the fraction of charges recovered during the stripping of lithium from the Li-Sn electrode. For cycling at a low current density of 0.4 mA/cm^2, the first two cycles showed coulombic efficiencies lower than 70% and the rest from 83 to 89%. Thus, lithium was stored in the Li-Sn electrode during the first two cycles for electrode development prior to cycling at a more or less constant efficiency at around 85% during most of the cycles. More than 200 cycles had been obtained with an average capacity of 140 mAh/g.

To study the effect of current density, the tin film electrode was cycled at constant current densities from 0.4 to 1.0 mA/cm^2. The change in the discharging capacity upon cycling at different current densities is shown in Fig. 9. The use of a current density higher than 0.4 mA/cm^2 leads to a rapid degradation of the discharging capacity upon cycling. Moreover, the tin alloy crystallites were found to expand and became irregular and loose when charging at a high cd of 1.0 mA/cm^2 for 20 cycles as shown by the SEM micrographs of the spent electrode (Fig. 10). However, when cycling at a low cd of 0.4 mA/cm^2, no obvious change of the morphology of the tin crystallites were obtained after 20 cycles, giving a more intact and regular crystal structure as shown in the SEM micrograph after 20 cycles. The difference in the crystal structures may account for the large difference observed in the rapid degradation in capacity when charging at a high cd (Fig. 9). Thus, the charging cd is recommended to be kept below 0.4 mA/cm^2.

In summary, the tin film electrode offers a better cycling performance at a low cd as compared to other metal alloy electrodes such as lithium-aluminum electrode that showed an appreciable problem of volume changing upon cycling.[10] This may be due to the special texture of the tin deposit film as shown in Fig. 3 that allows sufficient space between the tin crystal for the incorporation of lithium, thus mitigating a significant volume change during lithium deposition.

Table II. The performance of a tin film electrode cycled at a constant current density of 0.4 mA/cm^2.

Cycle number	Charging capacity (mAh/g)	Discharging capacity (mAh/g)	Coulombic efficiency (%)
1	541	271	50.1
2	206	139	67.5
3	170	149	87.6
4	169	140	82.8
5	165	137	83.0
10	156	133	85.3
20	157	139	88.5
30	150	128	85.3
40	148	122	82.4

Conclusions

In the search for a suitable negative electrode material for the lithium-ion battery in room temperature molten salt (RTMS), a new RTMS system containing 1-methyl-3-ethylimidazolium/$AlCl_3$/$SnCl_2$ (3:2:0.5) has been developed for the electrodeposition of tin on copper electrode. The tin film deposited at a potential more negative than −0.72 V under different temperatures produced tin crystallites with different surface morphologies and particle sizes, and showed widely different performances of the lithium cell (Sn (Cu)/LiCl buffered RTMS/lithium) assembled using LiCl buffered MEICl-$AlCl_3$ melts as the electrolyte. It was found that the tin film

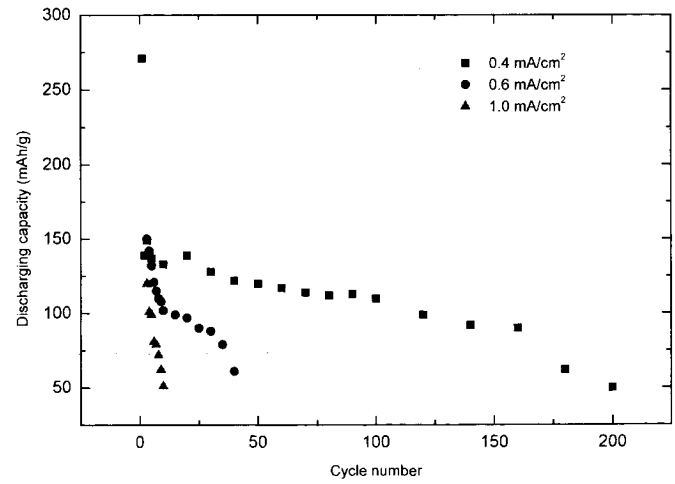

Figure 9. The discharging capacity for the tin film electrode cycling at different current densities.

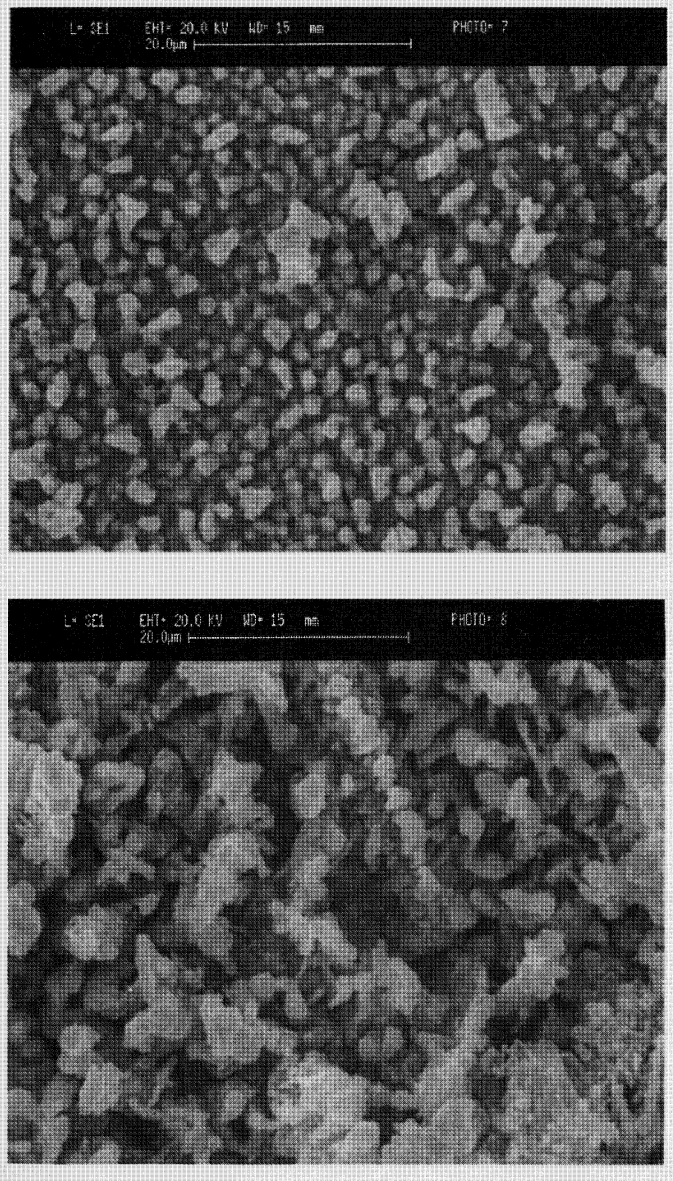

Figure 10. Scanning electron micrographs showing the morphology of the tin films after 20 cycles of charging-discharging at different current densities (a, top) 0.4 and (b, bottom) 1.0 mA/cm^2.

crystallites deposited at a temperature of 50°C or higher gave a desirable crystal structure and offered the best electrochemical performance as compared to those obtained at lower temperatures.

The results of cyclic voltammetry and galvanostatic cycling show the deposition of three major lithium-tin alloy phases corresponding to the two-phase transition for $LiSn/Li_7Sn_3$, $Li_{13}Sn_5/Li_7Sn_2$, and $Li_7Sn_2/Li_{22}Sn_5$ among the six intermediate phases identified in the Li/Sn system. Both the charging and discharging capacities were found to increase with the deposition of Li-Sn alloys with higher lithium activities. However, the irreversible capacity at the first cycle is also increased at the same time, indicating that more lithium was needed for the initial development of the tin film electrode when cycling at a higher voltage. When cycling at a high cd, the discharging capacity was found to decrease rapidly, producing loose, expanded, and irregular crystallites at the tin film electrode surface after 20 cycles at 1.0 mA/cm^2. When cycling at a low cd of 0.4 mA/cm^2, the performance of the tin film electrode was greatly improved, showing an average capacity of 140 mAh/g, a coulombic efficiency around 85%, and more than 200 cycles. The improvement is attributed to the deposition of small, regular, round tin crystallites that allows reversible insertion and removal of lithium from a more stable crystal structure deposited at high temperatures in the 1-methyl-3-ethylimidazolium/$AlCl_3/SnCl_2$ melt.

In summary, the tin film electrode offers a better cycling performance at a low cd as compared to other conventional metal alloy electrodes such as lithium-aluminum electrode. The improvement is attributed to the special texture of the tin deposited film that allows sufficient space between the tin crystals for the incorporation of lithium without a significant volume change during cycling.

Acknowledgments

We acknowledge the support of the Committee of the Hong Kong Research and Conference Grants and the Hong Kong Research Grants Council of the Hong Kong Special Administrative Region, China (HKU 302/93E) for this project.

The University of Hong Kong assisted in meeting the publication costs of this article.

References

1. Y. S. Fung and S. M. Chau, *J. Appl. Electrochem.*, **23**, 346 (1993).
2. Y. S. Fung and S. M. Chau, *Mater. Sci. Forum*, **73**, 677 (1991).
3. Y. S. Fung, *Trends Inorg. Chem.*, **5**, 117 (1998).
4. J. Fuller and R. A. Osteryoung, *J. Electrochem. Soc.*, **142**, 3632 (1995).
5. R. J. Gale and R. A. Osteryoung, *Inorg. Chem.*, **19**, 2240 (1980).
6. T. L. Riechel and J. S. Wilkes, *J. Electrochem. Soc.*, **139**, 977 (1992).
7. C. Scordilis-Kelly, J. Fuller, and J. S. Wilkes, *J. Electrochem. Soc.*, **139**, 694 (1992).
8. J. S. Wilkes, J. A. Levisky, R. A. Wilson, and C. L. Hussey, *Inorg. Chem.*, **21**, 1263 (1982).
9. C. Scordilis-Kelly and R. T. Carlin, *J. Electrochem. Soc.*, **140**, 1606 (1993).
10. Y. S. Fung and R. Q. Zhou, *J. Power Sources*, **81-82**, 891 (1999).
11. Y. S. Fung and R. Q. Zhou, in *Proceedings of 7th China-Japan Bilateral Conference on Molten Salts Chemistry and Technology*, p. 86 (1998).
12. Y. Idota, T. Kubota, A. Matsufuji, Y. Maekawa, and T. Miyasaka, *Science*, 276, 1395 (1997).
13. I. A. Courtney and J. R. Dahn, *J. Electrochem. Soc.*, **144**, 4045 (1997).
14. G. M. Ehrlich, C. Durand, X. Chen, and S. L. Suib, *J. Electrochem. Soc.*, **147**, 886 (2000).
15. Y. W. Xiao, J. W. Lee, A. S. Yu, and Z. L. Liu, *J. Electrochem. Soc.*, **146**, 3623 (1999).
16. G. M. Ehrlich, C. Durand, X. Chen, T. A. Hugener, F. Spiess, and S. L. Suib, *J. Electrochem. Soc.*, **147**, 886 (2000).
17. O. Mao and J. R. Dahn, *J. Electrochem. Soc.*, **146**, 414 (1999).
18. E. Peled and A. Ulus, in *Materials for Lithium-Ion Batteries*, C. Julien and Z. Stoynov, Editor, p. 585, Kluwer Academic Publishers, Norwell, MA (2000).
19. A. Armand, D. A. Fannin, Floreani, L. A. King, J. S. Wilkes, and J. L. Williams, *J. Phys. Chem.*, **88**, 2614 (1984).
20. Joint Committee on Powder Diffraction Standards, Powder Diffraction Data: from the Joint Committee on Powder Diffraction Standards Associateship at the National Bureau of Standards, 1st ed., 4-673, Washington, DC (1976).
21. C. J. Wen, and R. A. Huggins, *J. Solid State Chem.*, **35**, 376 (1980).